Joint Pathology Center
Veterinary Pathology Services

WEDNESDAY SLIDE CONFERENCE 2014-2015

Conference 1

3 September 2014

CASE I: Ex58B/Ex58G (JPC 3134882).

Signalment: A 7-year-old intact male German shepherd dog.

History: A 7-year-old intact male German shepherd dog was presented with hind limb paresis of 3 days duration and back pain. The referring veterinarian had treated the dog with prednisone and cephalexin for 3 days but the dog had deteriorated neurologically despite treatment. Neurological examination at presentation revealed paralysis of the right hind limb and paresis with minimal voluntary movement of the left hind limb. The dog appeared to be mainly in pain during postural shifts. All spinal reflexes were absent in the right hind limb. A weak withdrawal reflex was detected in the left hind limb. The neuroanatomic diagnosis was a lesion located in L4-S1 spinal cord segments and more severe on the right side. MRI examination was done 4 days post-admission and demonstrated an intramedullary increased signal intensity from the conus medularis to the level of L1. A surgical intervention was attempted but the dog's condition continued to deteriorate and it was

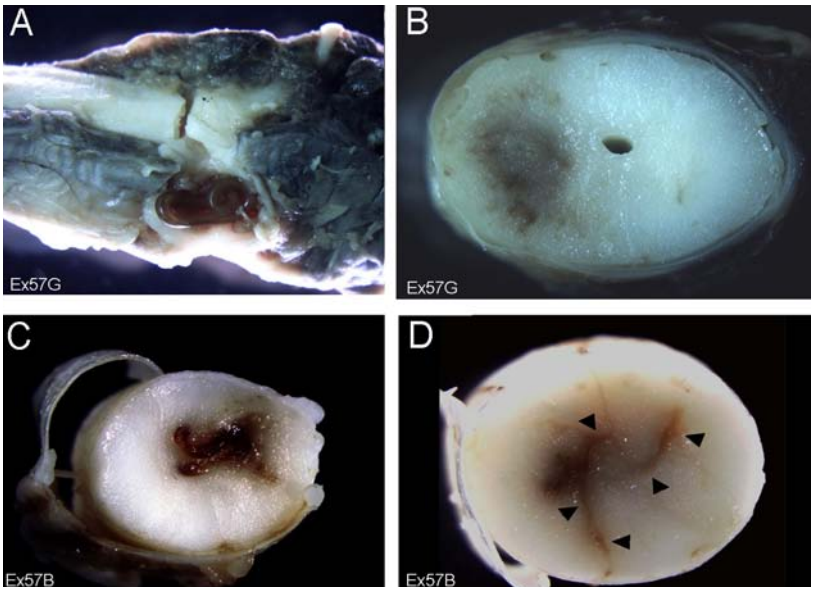

1-1. Lumbar spinal cord, dog: At necropsy, following incision of the dura, a single nematode was found embedded in the spinal parenchyma at L_1 –L_2 spinal segments on the left (Fig 1A). There were multiple, randomly distributed foci of hemorrhage and necrosis with or without cavitation involving the gray and white matter (Fig 1B). The lumbar segment was the most severely affected. Many necrohemorrhagic foci were continuous through multiple transverse sections and formed one or more tracts. The lesion was mostly located on the right side of the cord but moved to the left at L_1-L_2. Similar lesions were seen in the second case (Fig. 1C and D). (Photo courtesy of: Department of Veterinary Resources, Weizmann Institute, Israel. http://www.weizmann.ac.il/vet/

1-2. Lumbar spinal cord, dog: There are multiple areas of cavitation and necrosis (black arrows) within both the grey and white matter (black arrows). A transverse section of an adult spirurid nematode is present within one area of necrosis (green arrow). (HE 9X)

1-3. Lumbar spinal cord, dog: The adult S. lupi exhibits a thick smooth eosinophilic cuticle, polymyarian-coelomyarian musculature (black arrow), a pseudocoelom which contains abundant dark red material, large lateral chords (green arrow), and a large centrally located gastrointestinal tract. (HE 120X)

euthanized. Most of the slides submitted are from this case (Ex57G). Additional slides are from another dog with a history of acute progressive paraparesis and severe back pain beginning 3 days before presentation (Ex57B).

Gross Pathologic Findings: At necropsy, following incision of the dura, a single nematode was found embedded in the spinal parenchyma at L_1 –L_2 spinal segments on the left. Transverse sections of the spinal cord showed macroscopic changes from the caudal thoracic to the lumbar area. There were multiple, randomly distributed foci of hemorrhage and necrosis with or without cavitation involving the gray and white matter. The lumbar segment was the most severely affected. Many necrohemorrhagic foci were continuous through multiple transverse sections and formed one or more tracts. The lesion was mostly located on the right side of the cord but moved to the left at L_1-L_2. Similar lesions were seen in the second case.

Laboratory Results: CBC and serum biochemistry were unremarkable. Serological tests for *Toxoplasma gondii* and *Neospora caninum* were negative. Fecal flotation yielded *S. lupi* eggs. CSF analysis revealed mild mixed pleocytosis (40 cells/µl, reference interval: 0-8 cells/µl) with neutrophils (65%) and eosinophils (35%), and protein concentration of 22 mg/dl (RI: <25 mg/dl). Endoscopy demonstrated 3 typical *S. lupi* nodules in the caudal esophagus.

Histopathologic Description: In a random distribution within the white matter, there are several foci of necrosis and acute hemorrhage with mild gitter cell and variable neutrophilic infiltration. In the tissue around the tract, astrocytes show mild hypertrophy. Scattered vacuoles, some containing swollen axons (spheroids) and other cellular debris, are present in the white matter near the necrotic foci as well as further away. There is slight hemorrhage and mild gitter cell infiltration in the meninges within the ventral median fissure of one sample (lumbar intumescence). In another sample, there is widespread hemorrhage in the connective tissue external to the dura mater. There are several sections of a nematode with a smooth cuticle, coelomyarian-polymyarian muscles, large lateral hypodermal chords, abundant amphophilic to basophilic fluid in the pseudocoelom and an intestine composed of individual cuboidal cells, each with a prominent brush border. These features are typical of an adult spirurid, including *Spirocerca lupi.* Unfortunately, the parasite was dislodged during tissue processing. Sections from the second block (Ex57B) show a similar lesion but in this sample the tracts are present in the gray and white matter and there is mild to moderate inflammatory infiltration. Within one of the tracts there is a single transverse section at the level of the esophagus of a nematode with morphologic features as described above.

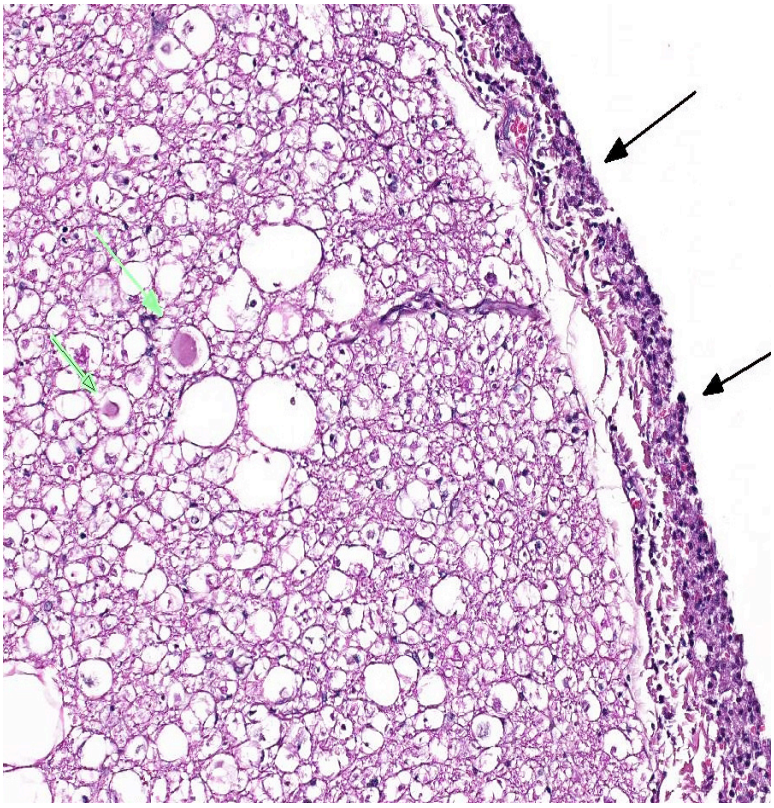

1-4. Lumbar spinal cord, dog: Within the lateral funiculi, there are moderate numbers of dilated axon sheaths which contain mildly to moderately swollen axons (spheroids) (green arrows), and the overlying meninges are expanded by moderate numbers of neutrophils, eosinophils, histiocytes and lymphocytes. (HE 144X)

Contributor's Morphologic Diagnosis: Spinal cord: Multifocal necrosis and hemorrhage with mild acute histiocytic and neutrophilic meningomyelitis and intralesional spirurid nematode.

Contributor's Comment: *Spirocerca lupi* is primarily a parasite of dogs. Its distribution is worldwide but it is most prevalent in warm climates. Adult parasites live in a nodular mass in the esophageal wall of the host. The female lays embryonated eggs which are transferred through a tract in the nodules and excreted with feces. The eggs are ingested by an intermediate host, corprophagus beetles, and develop to infective L3 within 2 months.

Carnivores are infected by ingestion of the beetles or a variety of paratenic hosts (birds, lizards, mice, rabbits etc.). In the carnivore host, the infective larvae penetrate the gastric mucosa and migrate within the walls of the gastric arteries to the thoracic aorta. About 3 months post-infection the larvae leave the aorta and migrate to the esophagus where they incite the development of fibro-inflammatory tissue (granulomas) as they mature to adults over the next 3 months. Lesions associated with *S. lupi* infestation are mainly due to migration and persistence of the parasite in tissues. Esophageal nodular masses (granulomas) and aortic scars and aneurysms are the most common lesions. Other lesions include spondylitis and spondylosis of the caudal thoracic vertebrae, neoplastic transformation of the esophageal granulomas, hypertrophic osteopathy, and aberrant migration into a wide variety of tissues including thoracic viscera, GIT, urinary system and subcutaneous tissue.[5]

More recently, several reports from Israel and South Africa describe aberrant migration into the spinal cord.[1,2,3] In one report (n=4) *S. lupi* was located in the extradural space and elicited signs typical of thoracolumbar IVD prolapse or spinal trauma.[2] In the remaining cases (n=5), tracts were present within the spinal cord as in the two cases used here.[2,3] Although confirmation of the diagnosis is difficult in cases which recover, the neurologists at the Veterinary School of the Hebrew University estimate that in the past 2-3 years, approximately 10-15 cases are seen annually (Dr. Orit Chai, personal communication). The reason for the increase in the occurrence of this form of canine spirocercosis is unknown but it may in part be attributable to failure in making the correct diagnosis in the past. Currently, a tentative diagnosis is based on the neurological signs, eosinophilic CSF pleocytosis and evidence of *S. lupi* infection in other tissues (by thoracic radiography, esophagoscopy and fecal floatation). The presenting signs of an acute nonsymmetrical paraparesis / plegia and high CSF eosinophil counts, observed in the present case, are similar to previously reported spinal intramedullary spirocercosis cases.[1]

The cause of aberrant migration of *S. lupi* is unknown. It has been suggested that aberrant migration occurs when a worm in the thoracic arterial wall enters the intercostal arteries and through their spinal branches arrives at the

extradural space. To enter the spinal cord it must then further penetrate the dura mater and the leptomeninges. The location reported in most intradural and extradural cases is T4-L1. In this region the aorta lies closely parallel to the vertebral column and the intercostal arteries supply the spinal branches that enter the spinal canal via the intervertebral foramina.[3]

Verminous encephalomyelitis may arise from aberrant wanderings of a parasite within its normal host (e.g., *Dirofilaria immitis* in the CNS of dogs and cats and *Strongylus vulgaris* in the brain of horses); or more commonly, infection of an aberrant host (e.g., *Paralephastrongylus tenuis*, the meningeal worm of white-tailed deer infesting sheep, goats and other herbivores). Other than regions where *S. lupi* is prevalent, cerebrospinal helminthosis is uncommon in dogs and cats. Nematodes, which may cause aberrant migration into the CNS of dogs include *Angiostrongylus cantonensis* in Australia, *Angiostrongylus vasorum* and *Dirofilaria immitis*.[6] There is a report of neurologic dysfunction in 3 dogs due to intracranial hemorrhage from consumptive coagulopathy associated with *Angiostrongylus vasorum* infection of the lung.[3]

JPC Diagnosis: Spinal cord: Meningomyelitis, necrotizing, eosinophilic, multifocal, marked, with adult spirurid nematode.

Conference Comment: This is an excellent example of aberrant migration in a normal host of a common and readily identifiable nematode. Conference participants reviewed the features of nematodes on histologic section of which they used the coelomyarian-polymyarian musculature that projects into the pseudocoelom, prominent lateral chords and eosinophilic material within the pseudocoelom in the present case to facilitate identification of a spirurid nematode, specifically *Spirocerca lupi.* Other spirurids of veterinary importance include: *Trichospirura leptostoma* inhabiting pancreatic ducts of the common marmoset, *Physaloptera* spp. residing in the stomach of many mammals, *Draschia megastoma* in the stomach of horses, and *Gongylonema* spp. found in the many different tissues and species.

The contributor provides an excellent overview of the complex pathogenesis of *Spirocerca* and appropriately conveys the tremendous variety of lesions associated with infection. Of significance is the pathognomonic lesion of thoracic spondylitis and its ability to induce malignant transformation, with esophageal fibrosarcoma or osteosarcoma being most characteristic.[7] This ability is not exclusive to *Spirocerca,* however. The acronym SOCCS-T is often used at JPC to facilitate remembering the following neoplasm-inducing parasites: *Spirocerca lupi, Opisthorchis felineus* (cholangiocarcinoma in cats and people), *Cysticercus fasciolaris* (hepatic sarcoma in rats), *Clonorchis sinensis* (cholangiocarcinoma in cats and people), *Schistosoma hematobium* (transitional cell carcinoma of urinary bladder in people) and *Trichosomoides crassicauda* (papillomas of rat urothelium).

Just as the contributor noted, it is the extensive migration of *Spirocerca* which most commonly causes lesions, as was the case in this dramatic example. Up to 80% of the section of spinal cord was affected in some slides, leading participants to speculate on how rapid the migration must have occurred to cause such extensive lesions in a relatively short period of time. Conference participants also discussed the clinicopathologic findings of pleocytosis, along with elevated neutrophils, eosinophils and protein, as expected findings of a cerebrospinal fluid analysis in this case. This is to contrast with an albuminocytologic dissociation, in which elevated protein levels does not accompany pleocytosis (seen with neoplastic or degenerative diseases such as Guillain-Barre syndrome in people).

Contributing Institution: Department of Veterinary Resources
Weizmann Institute, Israel
http://www.weizmann.ac.il/vet/

References:

1. Chai O, Shelef I, Brenner O, Dogadkin O, Aroch I, Shamir MH. Magnetic resonance imaging findings of spinal intramedullary sprocercosis. *Vet Radiol Ultrasound*. 2008;49:456-9.
2. Du Plessis CJ, Keller N, Millward IR. Aberrant extradural spinal migration of *Spirocerca lupi*: four dogs. *J Small Anim Pract.* 2007;48:275-278.
3. Dvir E, Perl S, Loeb E, et al. Spinal intramedullary aberrant Spirocerca lupi migration in three dogs. *J Vet Intern Med.* 2007;21:860-864.
4. Garosi LS, Platt SR, McConnell JF, Wray JD, Smith KC. Intracranial hemorrhage associated

with *Angiostrongylus vasorum* infection in three dogs. *J Small Anim Pract.* 2005;46:93-99.
5. Mazaki-Tovi M, Baneth G, Aroch I, et al. Canine spirocercosis: Clinical, diagnostic, pathologic and epidemiologic characteristics. *Vet Parasitol.* 2002;107:235-250.
6. Summers BA. Inflammatory diseases of the central nervous system. In: Summers BA, Cummings JF, de LaHunta A, eds. *Veterinary Neuropathology*. St. Louis, MO: Mosby-Year Book; 1995:159-162.
7. Van der Merwe LL, Kirberger RM, Clift S, Williams M, Keller N, Naidoo V. Spirocerca lupi infection in the dog: a review. *Vet J.* 2008;176(3): 294-309.

CASE II: L10-13908 (JPC 3167326).

Signalment: 11-year-old male rhesus macaque (*Macaca mulatta*).

History: This macaque was used for long-term visual and behavioral studies. A cranial head-stage implant was maintained on this animal for 4 years, which was associated with chronic purulent discharge. This purulent discharge was treated regularly with mechanical flushing and debridement, as well as anti-microbial therapy (based on routine culture and sensitivity results). No clinical signs were noted at the end of study period, although a physical examination just prior to barbiturate euthanasia revealed an enlarged liver upon abdominal palpation.

Gross Pathologic Findings: This macaque was presented dead in good body condition. Diffusely, the liver was enlarged (liver weight = 0.85 g; body weight = 6.8 kg), with rounded margins, and was pale red/tan and firm. A thick, viscous, pale green to pale yellow, opaque, odoriferous film of purulent material (biofilm) was noted in the subcutaneous tissues underneath the cranial head-stage implant. All other organs and tissues were within normal gross limits.

Laboratory Results: Mixed bacteria were isolated from the biofilm under the cranial head-stage implant, including *Staphylococcus* spp., *Streptococcus* spp., and *Enterococcus* spp. These were all resistant to most antimicrobials except enrofloxacin and ciprofloxacin.

Histopathologic Description: Sections of liver are examined. There is extensive effacement of normal hepatic lobular architecture due to the presence of massive amounts of amorphous, homogenous sheets of eosinophilic hyaline acellular material that appears to originate in and expand the space of Disse. This material is congophilic and displays bright-green birefringence when viewed under polarized light. Multifocally and extensively, the amyloid deposits in the space of Disse often expand outward to involve adjacent sinusoidal spaces (resulting loss of the sinusoidal lumen), and the amount of amyloid present results in massive to total loss of normal hepatocytes and hepatic lobular architecture, with remaining hepatocytes appearing sparse, compacted/atrophied, and displaced into thin, often tortuous hepatic cords. Occasional portal triads and central veins are still recognizable.

Contributor's Morphologic Diagnosis: Liver, hepatic amyloidosis, severe, diffuse, chronic.

Contributor's Comment: **Amyloid** refers to a heterogenous group of protein fibrils that share a common ultrastructural feature, namely that extracellular cross polymerization of the fibrils results in the formation of insoluble β-pleated sheets.[1] Biochemically, at least 20 different types of amyloid protein have been discovered in humans and animals. **Amyloidosis** refers to human and animal diseases that are characterized by the extracellular deposition of amyloid in various tissues, often resulting in dysfunction of compromised organs.[1]

Amyloidosis can be classified by the biochemical composition of the amyloid protein involved.[9] Amyloidosis can also be classified on the basis of whether it results from a primary or secondary disease process, and whether amyloid deposition is localized to one tissue or multiple tissues (systemic).[10] More typically, classification of amyloidosis often reflects a combination of all these systems.[10]

The two most traditionally recognized forms of systemic amyloidosis in humans and animals are:

1. **Primary amyloidosis (AL),** characterized by the deposition of immunoglobulin light chain that is overproduced by plasma cell/B-cell dyscrasias (e.g., multiple myeloma, B-cell proliferations).[1,10]

2. **Secondary/reactive systemic amyloidosis (AA),** characterized by the deposition of serum amyloid A (SAA), is produced as a liver-derived acute phase protein as part of inflammatory processes. In this form, a chronic-active inflammatory process usually occurs that results in sustained production of SAA, but a defect in the degradation of SAA (perhaps due to excessive levels of SAA that overwhelm the enzymatic degradation pathway; a defect in the enzymatic degradation pathway; or a structural difference of the SAA fibril that

2-1. Liver, rhesus macaque: The liver was diffusely enlarged (liver weight = 0.85 g; body weight = 6.8 kg) with rounded margins. (Photo courtesy of: Veterinary Services Center, Department of Comparative Medicine, Stanford School of Medicine (http://med.stanford.edu/compmed/). (HE 0.63X)

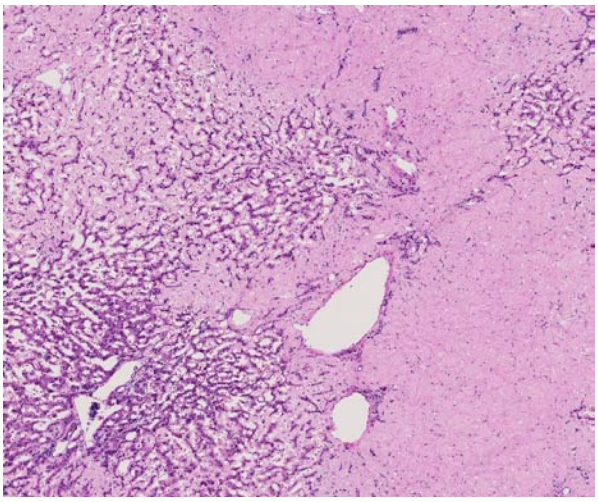

2-2. Liver, rhesus macaque: Large areas of amyloid surround and replace hepatic parenchyma. (HE 34X)

makes it resistant to degradation), leading to the development of AA amyloidosis.[1,10]

There are several types of amyloidosis that occur in macaques, the major type being **secondary/ reactive amyloidosis (AA)**. This has been reported in rhesus macaques, in association with enterocolitis (usually associated with *Shigella* spp. infection),[2,4] osteoarthritis,[2,3,4] and chronic indwelling venous catheters.[6] In pig-tailed macaques, secondary/reactive amyloidosis is associated with enterocolitis, retroperitoneal fibromatosis, and glomerulonephritis.[10] In most reported cases, advancing age is a predisposing factor for the deposition of AA amyloid.[2,3,4,6,12,15] The deposition can be systemic or (more rarely) localized, with typical tissues that are affected being small intestines, liver, spleen, and kidney.[8] A notable localized form of secondary/reactive amyloidosis appears to be **intestinal amyloidosis (AA),** which has been reported in cynomolgus macaques[14] and pig-tailed macaques.[7] In this form, there is localized deposition of AA amyloid in the lamina propria of the small intestines (and less often, the large intestines), and may occur as an incidental lesion in aged macaques.[7,14] However, it is more commonly linked to a clinical syndrome of weight loss and diarrhea resulting from protein-losing enteropathy.[7]

Other distinct forms of amyloidosis in macaques include:

- **Cerebral amyloidosis (Aβ),** which involves the deposition of amyloid β protein precursor as either plaques (senile amyloid plaques) within the neuropil and/ or as deposits within vessels walls (cerebral amyloid angiopathy) of the brain. This has been reported in rhesus macaques[14] and cynomolgus macaques[11] which are used animal models for Alzheimer's disease research.

- **Pancreatic islet amyloidosis (AIAAP),** where amylin (islet-associated polypeptide) accumulation is localized to endocrine pancreatic islets, is often associated with diabetes mellitus. This has been documented in cynomolgus macaques[5,16] and Celebes-crested macaques,[5] and provide a nonhuman primate model for diabetes mellitus research.

In general, clinical presentation of macaques affected with secondary/reactive amyloidosis reflects the type of tissues that are involved, the amount of amyloid involved, and the primary inciting causes (if any can be identified) that may be involved. For example, amyloidosis involving the gastrointestinal tract or liver can present similarly with weight loss due to hypoproteinemia (via protein-losing enteropathy and decreased hepatic function respectively). Intestinal amyloidosis may also present with diarrhea, due

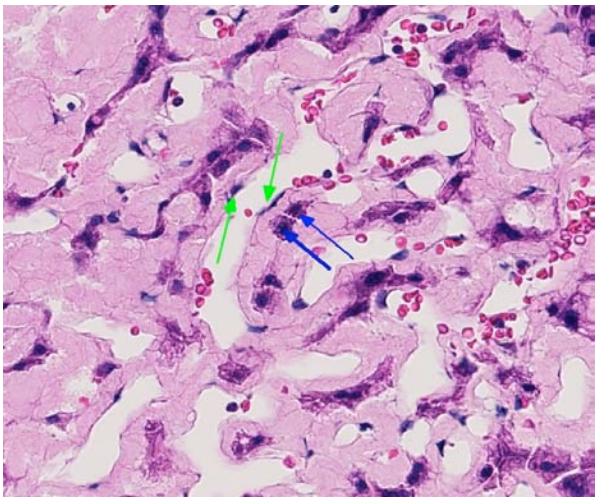

2-3. Liver, rhesus macaque: Amyloid fills the space of Disse between hepatocytes (blue arrows) and endothelial cells (green arrows). (HE 284X)

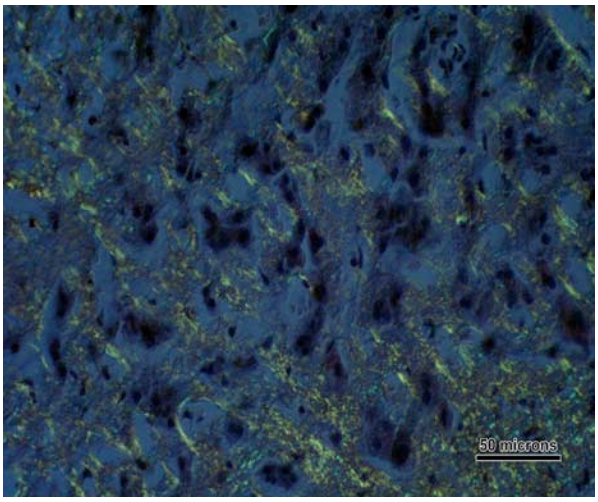

2-4. Liver, rhesus macaque: Material within the space of Disse is congophilic and displays bright-green birefringence when viewed under polarized light. (HE 400X)

to both the presence of amyloid with the mucosa and the primary instigating pathogen (e.g., shigellosis).

Noninvasive, antemortem diagnosis of secondary/reactive amyloidosis in macaques is difficult. Clinical biochemistry studies of macaques with amyloidosis have consistently revealed significant elevations in γ-glutamyl transferase, aspartate aminotransferase, and alkaline phosphatase, and significant decreases in total protein and albumin.[6,8,9] Serum electrophoresis may reveal hypergammaglobulinemia (polyclonal gammopathy) as well.[6] Immunoassays have also revealed elevations in SAA early in the disease course and elevations in macrophage colony-stimulating factor later in the disease course.[9] Diagnostic imaging (e.g., radiography, magnetic resonance imaging) can be used to evaluate hepatomegaly if the liver contains significant amounts of amyloid, but are very insensitive for mild and subclinical cases.[8]

The diagnosis and differentiation of secondary/reactive amyloidosis can be achieved using several methods:

1. **Gross pathology** is often unrewarding in mild to moderate or subclinical cases. In severely affected animals however, gross examination may reveal enlarged livers that are often described as pale, friable to firm, and waxy; prominent white pulp areas on the cut surfaces of spleens; or thickened gastrointestinal mucosa. Chronically-affected animals may also display emaciation associated with weight loss.[2,3,4,8,12]

2. **Histopathology** of tissues obtained as biopsy specimens or from necropsy is the traditional gold standard for diagnosis of secondary/reactive amyloidosis. Amyloid appears as amorphous, acellular, homogenous eosinophilic extracellular material on H&E sections, and occurs most prominently in the space of Disse in the liver, the follicular white pulp areas in the spleen, the lamina propria of the gastrointestinal tract, the medullary interstitium of the kidneys, and the corticomedullary junction of the adrenal glands.[2,3,4,8,12]

   Other histochemical and immunohistochemical stains can be performed to definitively confirm the presence of AA amyloid in tissues. The most commonly used histochemical stain is Congo red. Like all amyloid, AA amyloid appears orange to rosy-pink with Congo red staining, and will display bright green birefringence when examined with polarized light. However, AA amyloid (in contrast to other types of amyloid) loses its congophilic and birefringence properties if treated with potassium permanganate prior to Congo Red staining.[2,3,12] Antibodies for most

types of amyloid proteins (including AA amyloid) are commercially available.

We believe that the case of hepatic amyloidosis presented here represents severe localized secondary/reactive amyloidosis in the liver. Observable amyloid deposition was not noted in all other tissues examined histologically. The cause of the amyloidosis was most likely the chronic infection of the subcutaneous tissues under the cranial head-stage implant ("peri-implantitis") in this macaque, which is a common cause of secondary/reactive amyloidosis in macaques observed in our institution.

JPC Diagnosis: Liver, space of Disse: Amyloidosis, diffuse, severe, with marked hepatocellular atrophy and loss.

Conference Comment: The contributor provides an excellent overview of amyloidosis with emphasis on the variety of manifestations in nonhuman primates. This case is an exceptional example of hepatic amyloidosis, as it nicely illustrates the expansion of the perisinusoidal space with amyloid. This area, known as the space of Disse, is the narrow space between the plates of hepatocytes and sinusoidal lining cells where amyloid is known to accumulate within the liver. For reviewing the important ultrastructural appearance of amyloid with its randomly oriented fibrils in this characteristic location, we refer the reader to the EM case from the 2013 WSC (conference 6, case 4).

Conference participants noted the severity of the lesion in this case and were amazed as to the lack of clinical signs in this animal. Participants agreed the source of amyloid is most likely due to the chronic inflammation in response to the implant, resulting in reactive amyloid A (AA). Not likely applicable in this instance, but of academic interest, is the recent evidence suggesting AA amyloidosis is transmissible, both within and between species.[13] While currently only demonstrable experimentally, the possibility of amyloid transmission between species and the presence of amyloid in skeletal muscle of food animals such as poultry and cattle suggests a potential public health concern worthy of further investigation.

Contributing Institution: Veterinary Services Center
Department of Comparative Medicine
Stanford School of Medicine
(http://med.stanford.edu/compmed/)

References:

1. Addie DD, Jarrett O. Feline coronavirus infections. In: Greene CE, ed. *Infectious Diseases of the Dog and Cat*. 3rd ed. St. Louis, MO: Saunders; 2006:91-100.
2. Bradshaw JM, Pearson GR, Gruffydd-Jones TJ. A retrospective study of 286 cases of neurological disorders of the cat. *J Comp Path.* 2004;131:112–120.
3. Brown CC, Baker DC, Barker IK. Alimentary system. In: Maxie MG, ed. *Jubb, Kennedy, and Palmer's Pathology of Domestic Animals*. Vol. 2. 5th ed. London, UK: Saunders Elsevier; 2007:290-293.
4. Diaz JV, Poma R. Diagnosis and clinical signs of feline infectious peritonitis in the central nervous system. *Can Vet J.* 2009;50(10):1091–1093.
5. Foley JE, Leutenegger C. A review of coronavirus infection in the central nervous system of cats and mice. *J Vet Intern Med.* 2001;15(5):438–444.
6. Foley JE, Lapointe JM, Koblik P, Poland A, Pedersen NC. Diagnostic features of clinical neurologic feline infectious peritonitis. *J Vet Intern Med.* 1998;12(6):415–423.
7. Giori L, Giordano A, Giudice C, Grieco V, Paltrinieri S. Performances of different diagnostic tests for feline infectious peritonitis in challenging clinical cases. *J Small Anim Pract*. 2011;52:152-157.
8. Gunn-Moore DA, Reed N. CNS disease in the cat: current knowledge of infectious causes. *J Fel Med Surg*. 2011;13(11):824–836.
9. Keel SB, Abkowitz JL. The microcytic red cell and the anemia of inflammation. *N Engl J Med*; 2009;361(19):1904-1906.
10. Kent M. The cat with neurological manifestations of systemic disease. Key conditions impacting on the CNS. *J Fel Med Surg*. 2009;11(5):395–407.
11. Kipar A, Meli ML. Review of feline infectious peritonitis: Still an enigma? *Vet Pathol*. 2014:51(2):505-526.
12. MacLachlan NJ, Dubovi EJ. *Fenner's Veterinary Virology*. 4th ed. London, UK: Academic Press; 2011:393-412.

13. Murakami T, Ishiguro N, Higuchi K. Transmission of systemic AA amyloidosis in animals. *Vet Pathol.* 2014;51(2):363-371.
14. Myrrha LW, Miquelitto Figueira Silva F, Fernandes de Oliveira Peternelli E, Silva Junior A, Resende M, Rogéria de Almeida M. The paradox of feline coronavirus pathogenesis: a review. *Adv Virol*. 2011;2011:1-8.
15. Rand JS, Parent J, Percy D, Jacobs R. Clinical, cerebrospinal fluid, and histological data from twenty-seven cats with primary inflammatory disease of the central nervous system. *Can Vet J.* 1994;35(2):103–110.
16. Sharif S, Suri Arshad S, Hair-Bejo M, Rahman Omar A, Allaudin Zeenathul N, Alazawy A. Diagnostic methods for feline coronavirus: a review. *Vet Med Int*. 2010;2010:1-7.
17. Singh M, Foster DJ, Child G, Lamb WA. Inflammatory cerebrospinal fluid analysis in cats: Clinical diagnosis and outcome. *J Fel Med Surg.* 2005;7(2):77–93.
18. Tsai HY, Ling-Ling C, Chao-Nan L, Bi-Ling S. Clinicopathological findings and disease staging of feline infectious peritonitis: 51 cases from 2003 to 2009 in Taiwan. *J Feline Med Surg.* 2010;13:74-80.
19. Wise AG, Kiupel M, Maes RK. Molecular characterization of a novel coronavirus associated with epizootic catarrhal enteritis (ECE) in ferrets. *Virology.* 2006;349:164–174.

CASE III: 2013910414 (JPC 4048844).

Signalment: 11-year, 8-month-old male Papillon, dog (*Canis familiaris*).

History: The dog had been bitten on the left femoral skin, and a 12 x 16 mm dermal mass formed at first in the region. The mass was covered with crust. On fine needle aspiration, only lipocytes were found. He was fitted with an Elizabethan collar to prevent self-trauma and was topically treated with antibiotics and steroids with no clinical improvement. The mass increased in size for two years.

Gross Pathology: The masses were arranged in a pattern resembling a horse's hoof, and some masses were ulcerated.

Laboratory Results: None

Histopathologic Description: The multiple variably sized masses are present in the dermis and subcutis, with multiple small masses around large masses. Various-sized swollen peripheral nerve fascicles are observed in each mass, with perineurial hyperplasia. In the large mass, perineurial hyperplasia and fibrosis is more remarkable. Swollen nerve fascicles in each mass consist of thin, unmyelinated nerves with hypertrophic Schwann cells and a thickened perineurium.
Immunohistochemically, nerve fascicles include neurofilament-positive axons with GFAP-positive Schwann cells. Hyperplastic perineurium is positive for type 4 collagen and nerve growth factor receptor (NGFR). Small nerve fibers, which are positive for GFAP and PGP9.5, are included in hyperplastic perineurium. These lesions show no significant proliferative activity based on Ki-67 staining.

Contributor's Morphologic Diagnosis: Skin: Multiple traumatic neuroma with swollen nerve fascicles and perineurial hyperplasia.

Contributor's Comment: The present case was characterized by swollen peripheral nerve fascicles with perineurial hyperplasia and fibrosis. Each nerve fascicle consisted of thin to unmyelinated nerve fibers, including axons and Schwann cells. Axons in swollen nerve fascicles and hyperplastic perineurium had Schwann cells as well as normal nerve fibers, suggesting a non-neoplastic lesion. The lack of proliferative activity also indicated that our case was non-neoplastic. The histological features resembled traumatic neuroma except swollen large-sized nerve fascicles and perineurial hyperplasia. Perineurial hyperplasia and fibrosis were observed in Morton's neuroma, which is one subtype of traumatic neuroma in humans. With clinical findings and histological features, it was suggested that peripheral nerves of affected area were the result of self-inflicted injury. Thus, the present case was diagnosed as unique subtype of traumatic neuroma.

Traumatic neuroma is a reactive and non-neoplastic proliferative nerve disease to injury or surgery at the proximal end of an injured peripheral nerve.[6,16] In the dog, it has been reported following tail docking.[7] Microscopically, small nerve fascicles including axons with their investiture of myelin, Schwann cells, and fibroblasts proliferate with abundant fibrous stroma.[16] Many axons were seen in a parallel distribution within fascicles.[4] Ascertaining the presence of axons by immunohistochemical examination is useful in distinguishing "non-neoplastic" neuroma from neoplasms such as Schwanoma and neurofibroma.[2]

Morton's neuroma (localized interdigital neuritis) is not a true tumor and one subtype of traumatic neuroma caused by chronic or repeated mild trauma to the region. The lesion is commonly seen in the interdigital plantar nerve of third and fourth toes in women.[13,16] Histologically, proliferative changes characterize traumatic neuromas, whereas degenerative changes are the hallmark of Morton's neuroma. As the lesion progresses, the fibrosis becomes marked and envelops the epineurium and perineurium in a concentric fashion and even extends into the surrounding tissue.[8,16] Similarly, when hands are injured due to vibration from hand held power tools, demyelination and perineurial and endoneural fibrosis can develop in the nerves in fingers and wrists.[14]

The present case needs to be differentiated from a neoplasm because the histological features of hyperplastic perineurium with fibrosis are similar to Schwannoma, neurofibroma and perineurioma. Schwannoma or neurofibroma with plexiform pattern most closely resembled the present case.[13,16] With continued growth in these tumors, the

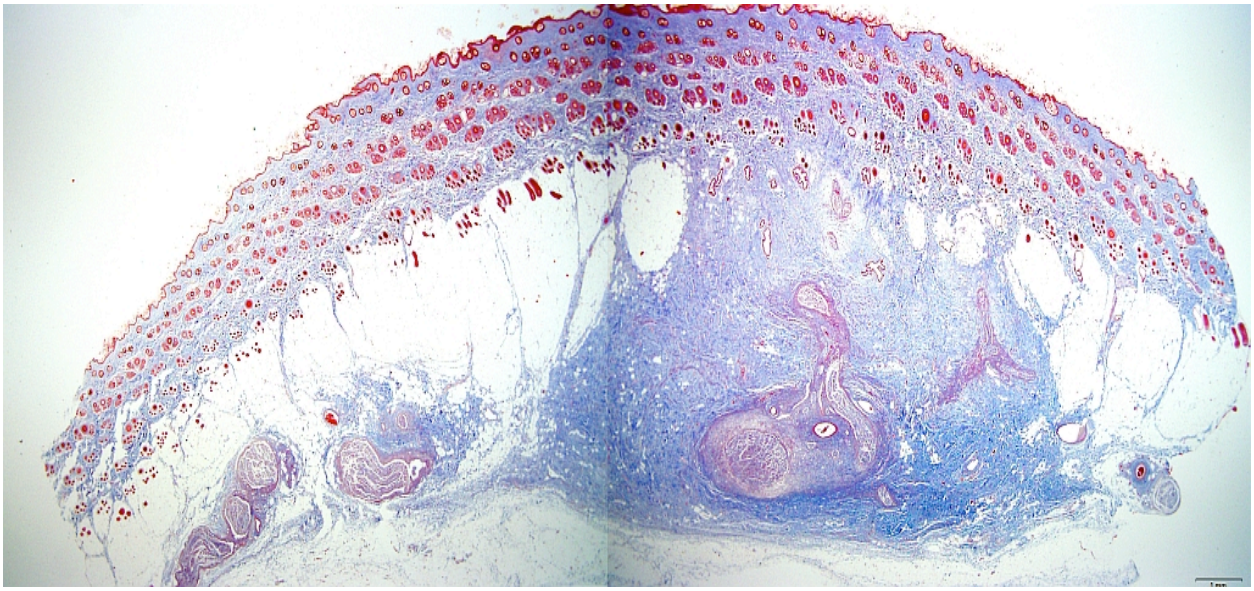

3-1. Haired skin, dog: This tiled image shows the extent of a neuroma that arose over two years following a dog bite at the site. The mass is composed of clusters of large caliber nerve fibers surrounded by fibrous connective tissue. (Masson's Trichrome, 0.3X) (Photo courtesy of: Department of Pathology, Faculty of Pharmaceutical Sciences, Setsunan University, 45-1 Nagaotohge-cho, Hirakata, Osaka 573-0101, Japan. http://www.setsunan.ac.jp/~p-byori/)

fascicular components infiltrate surrounding soft tissue. The pathological features are similar to the present case at first. Schwannoma is composed of mainly Schwann cells with characteristic patterns and containing few axons. Neurofibroma consists of a mixture of Schwann cells, axons and fibroblasts, and the number of axons is very low.[13,15] Perineuroma has multiple forms: intraneural, extraneural, sclerosing, reticular, and hybrid features with neurofibroma or schwannoma.[16] Intraneural perineurioma is composed of concentric layers of perineurial cells ensheathing an axon and Schwann cell. Extraneural perineurioma is an extremely elongated spindle cell lesion arranged in parallel bundles. In the present case, perineurial cells do not proliferate inside nerve fascicles, but increase in the margin of nerve fascicles, which is a normal site. Additionally, many nerve fibers randomly proliferate in hyperplastic perineurium.

Human perineurial cells are immunoreactive for epithelial membrane antigen (EMA), but negative for S-100.[4,11,13,16,17] GFAP and S100 commonly stain Schwann cells. Thus, immunostaining for these proteins is always used to distinguish between perineurial cell and Schwann cells. However, in canine perineurioma, the tumor cells are negative for EMA.[10] The basement membrane between perineurial cells are positive for type 4 collagen and laminin.[16] Additionally, positive staining for type 4 collagen and NGFR can help identify nerve origin.[3,4] Thus, our results indicate that immunohistochemistry for type 4 collagen and NGFR might be useful for identifying perineurial cells of the dog.

JPC Diagnosis: Haired skin: Neuroma.

Conference Comment: This case provides an interesting diagnostic exercise in distinguishing neoplastic from non-neoplastic proliferative peripheral nerve lesions. Neuroma is a well-known entity, which has been described in the literature for over 50 years.[15] Its name perhaps inappropriately implies neoplasia, as the contributor previously discusses.

Neuroma development following trauma, most commonly observed subsequently to tail-docking or digital neurectomy in horses, is presumed to arise when the normal regenerative growth of a disrupted nerve fiber encounters a physical obstruction such as scar tissue.[7] This results in a haphazard arrangement of axons and disorganized microfascicular architecture, observed in this case as numerous Schwann cells and few axons haphazardly arranged and surrounded by a variably thick fibrotic perineurium.

The classification of a non-neoplastic lesion implies the proliferating cell population still

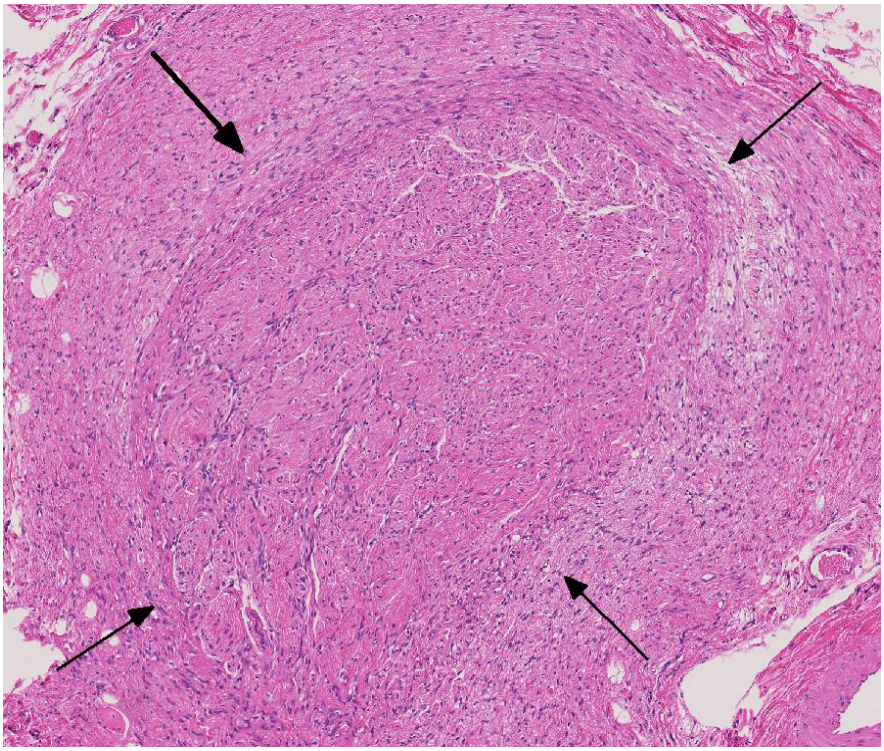

3-2. Haired skin, dog: Proliferating nerve bundles are surrounded by a markedly thickened perineurium. (HE 61X)

possesses control over its growth cycle and/or stability of its genome. This is an opportunity for the reader to review the hallmarks of neoplasia and independently consider whether any of these may apply in this case. The following six hallmarks are acquired in succession and lead to cells becoming neoplastic and eventually malignant: sustained proliferative signaling, evasion of growth suppressors, resisting cell death, enabling replicative immortality, induction of angiogenesis and the activation of invasion and/or metastasis. Recently, two further hallmarks have been added: the reprogramming of energy metabolism and evasion of the immune response. Two characteristics described as crucial to the acquisition of these hallmarks are genomic instability and tumor-promoting inflammation. When mutations are permanently acquired in the genome, the cell may develop a selective advantage that enables its outgrowth and eventual dominance in the local environment that may be fueled by growth and survival factors supplied by secondary inflammatory cells.[9]

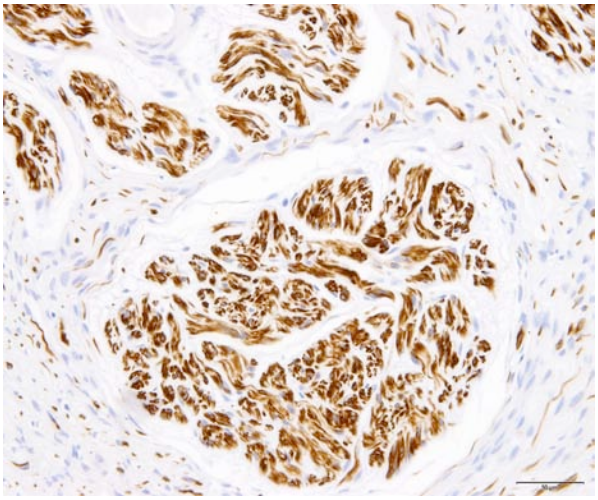

3-3. Haired skin, dog: Nerve fibers demonstrate strong intracytoplasmic immunostaining for anti-glial fibrillary acidic protein. (GFAP 100X)

Conference participants reviewed the most common neural tumors of domestic animals. Schwannomas, which originate from a single nerve and extend in conjunction with but external to it, facilitates its involvement with plexus arrangements such as the brachial plexus and other common sites including the heart base, spinal nerve roots and the tongue.[12] Neurofibromatosis is a well-recognized variant of Schwannomas observed in cattle in which multiple sites are involved. Peripheral nerve sheath tumors are of controversial origin, but often found on the distal limbs of dogs and graded according to soft tissue sarcoma criteria.[5] Ganglioneuromas are rare tumors reported in many species and are composed of ganglion and glial cells. Ganglioneuroblastomas are similar but are composed of poorly differentiated ganglion cells with more atypia.[12]

Contributing Institution: Department of Pathology, Faculty of Pharmaceutical Sciences, Setsunan University, 45-1 Nagaotohge-cho, Hirakata, Osaka 573-0101, Japan
http://www.setsunan.ac.jp/~p-byori/

References:

1. Antunes SL, Chimelli L, Jardim MR, et al. Histopathological examination of nerve samples from pure neural leprosy patients: Obtaining maximum information to improve diagnostic efficiency. *Mem Inst Oswaldo Cruz*. 2012;107(2): 246-253.

2. Arishima H, Takeuchi H, Tsunetoshi K, Kodera T, Kitai R, Kikuta K. Intraoperative and pathological findings of intramedullary amputation neuroma associated with spinal ependymoma. *Brain Tumor Pathol*. 2013;30:196-200.

3. Chijiwa K, Uchida K, Tateyama S. Immunohistochemical evaluation of canine peripheral nerve sheath tumors and other soft tissue sarcomas. *Vet Pathol.* 2004;41:307-318.

4. Chrysomali E, Papanicolaou SI, Dekker NP, Regezi JA. Benign neural tumors of the oral cavity: a comparative immunohistochemical study. *Oral Surg Oral Med Oral Pathol Oral Radiol Endod*. 1997;84:381-390.

5. Dennis MM, McSporran KD, Bacon NJ, Schulman FY, Foster RA, Powers BE. Prognostic factors for cutaneous and subcutaneous soft tissue sarcomas in dogs. *Vet Pathol.* 2011;48(1):73-84.

6. Ginn PE, Mansell JL, Rakich PM. Neoplastic and reactive disease of the skin and mammary glands. In: *Jubb & Kennedy Pathology of Domestic Animals*. Vol. 1. St Louis, MO: Sanders Elserver; 2006:761-767.

7. Gross TL, Carr SH. Amputation neuroma of docked tails in dogs. *Vet Pathol*. 1990;27:61-62.

8. Guiloff RJ, Scadding JW, Klenerman L. Morton's metatarsalgia. Clinical, electrophysiological and histological observations. *J Bone Joint Surg Br.* 1984;66:586-591.

9. Hanahan D, Weinberg RA. Hallmarks of cancer: the next generation. *Cell*. 2011;144:646-674.

10. Higgins RJ, Dickinson PJ, Jimenez DF, Bollen AW, Lecouteur RA. Canine intraneural perineurioma. *Vet Pathol*. 2006;43:50-54.

11. Hirose T, Tani T, Shimada T, Ishizawa K, Shimada S, Sano T. Immunohistochemical demonstration of EMA/Glut1-positive perineurial cells and CD34-positive fibroblastic cells in peripheral nerve sheath tumors. *Mod Pathol.* 2003;16:293-298.

12. Maxie MG, Youssef S. Nervous system. In: *Jubb & Kennedy Pathology of Domestic Animals*. Vol. 1. St Louis, MO: Sanders Elsevier; 2006:455.

13. Rosai J. Tumors and tumor-like conditions of peripheral nerves. In: *Rosai and Ackerman's Surgical Pathology*. St. Louis, MO: Elsevier Mosby; 2004:2263-2271.

14. Stromberg T, Dahlin LB, Brun A, Lundborg G. Structural nerve changes at wrist level in workers exposed to vibration. *Occup Environ Med*. 1997;54:307-311.

15. Swanson HH. Traumatic neuromas: a review of the literature. *Oral Surg Oral Med Oral Pathol.* 1961;14:317-326.

16. Weiss SW, Goldblum GJ. Benign tumors of peripheral nerves. In: *Enzinger and Weiss's Soft Tissue Tumors*. St. Louis, MO: Mosby; 2013:784-854.

17. Yamaguchi U, Hasegawa T, Hirose T, et al. Sclerosing perineurioma: a clinicopathological study of five cases and diagnostic utility of immunohistochemical staining for GLUT1. *Virchows Arch*. 2003;443:159-163.

CASE IV: 07N1149 (JPC 3100109).

Signalment: Neonate female American Quarter horse, *Equus caballus.*

History: The foal gasped at birth then stopped breathing. The foal was dead on arrival to the University of California, Davis Veterinary Medical Teaching Hospital. Intubation was unsuccessful.

Gross Pathological Findings: The mucous membranes of the oral cavity were diffusely tinged blue (cyanosis). Approximately 20% of the pulmonary parenchyma was aerated and the remaining lung tissue was atelectic (fetal atelectasis). Foci of epicardial hemorrhages were present on the right ventricle, adjacent to the atrio-ventricular junction. Pinpoint hemorrhages were scattered throughout the thymus and on the mucosal surface of the esophagus.

Histopathologic Description: Skeletal muscle (diaphragm, semitendinosis): Within numerous swollen myofibers are discrete glassy to compact granular, lightly basophilic, oval to variably shaped and sized inclusion bodies that are up to approximately 50 µm in length. The inclusions disrupt and/or replace the normal cytoplasmic myofibril architecture.

Heart: Intracytoplasmic inclusions, similar to those previously described, are within numerous variably swollen and disrupted myocytes.

Brainstem: A few to moderate numbers of large neuronal cell bodies contain intracytoplasmic inclusion bodies, similar to those previously described.

Contributor's Morphologic Diagnoses: 1. Heart, Skeletal muscle (diaphragm, intercostal, thigh): Severe multifocal myofiber degeneration with intracytoplasmic inclusions.
2. Brainstem: Moderate neuronal degeneration with intracytoplasmic inclusions.

Laboratory Results: Period acid-Schiff staining of formalin-fixed, paraffin-embedded tissues collected at the time of necropsy, sectioned at 5 µm, show intensely PAS-positive, large intracytoplasmic inclusions within swollen skeletal muscle fibers (tongue, diaphragm, intercostal, semitendinosis, quadricep), in cardiac myocytes, and within large neuronal cell bodies in the brainstem.

Genotyping was performed at the Veterinary Genetics Laboratory at the University of California, Davis. DNA used for analysis was isolated from formalin fixed paraffin embedded skeletal muscle tissue. Analysis showed the foal to be homozygous for the single nucleotide polymorphism responsible for glycogen branching enzyme deficiency.

Transmission electron microscopy was performed on formalin fixed skeletal muscle and brainstem at the California Animal Health and Food Safety Laboratory, Davis Branch. Transmission electron

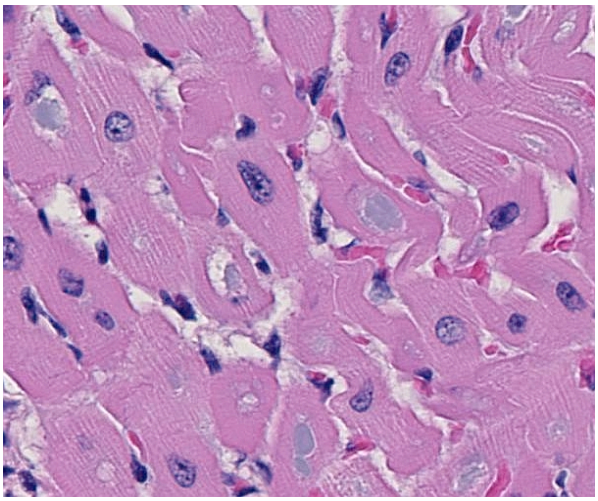

4-1. Heart, foal: Cardiomyocytes contain one or multiple amphophilic cytoplasmic inclusions. (HE 400X)

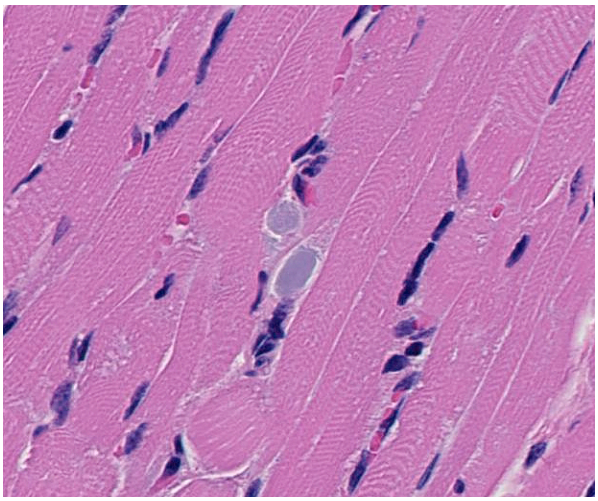

4-2. Skeletal muscle, foal: Rhabdomyocytes contain one or multiple amphophilic cytoplasmic inclusions. (HE 400X)

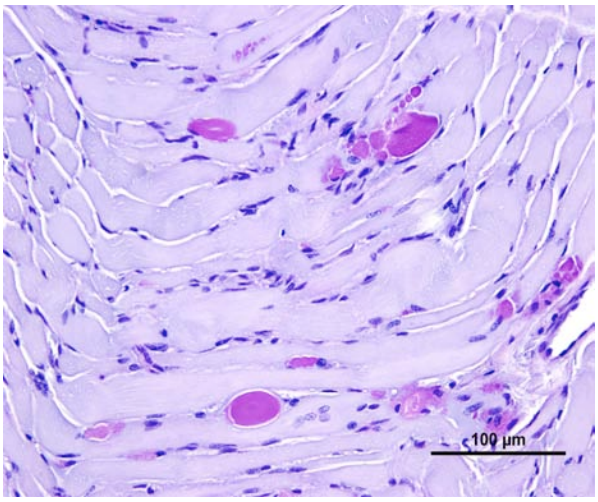

4-3. Skeletal muscle, foal: PAS-positive inclusions displace myofibrils within swollen muscle fibers. (PAS 200X) (Photo courtesy of: University of California, Davis, Veterinary Medical Teaching Hospital, VM3A, Anatomic Pathology, One Shields Avenue, Davis, CA 95616 http://www.vetmed.ucdavis.edu/pmi/)

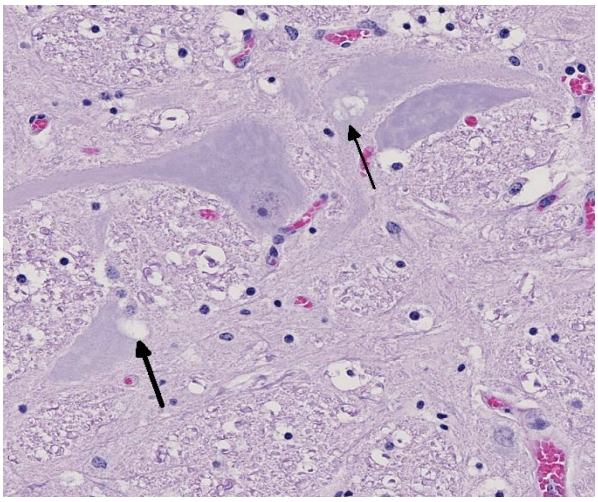

4-4. Brainstem, foal: Brainstem neurons contain multifocal intracytoplasmic inclusions. (HE 400X)

microscopy revealed large electron dense filamentous to granular inclusions in degenerate skeletal muscle fibers. Similar inclusions are seen within degenerate neuronal cell bodies within the brainstem.

Contributor's Comment: Glycogen branching enzyme deficiency, or glycogen storage disease IV, is a fatal hereditary condition that occurs in American Quarter horse and American Paint horse lineages. The inheritance pattern is autosomal recessive. The genetic mutation responsible for this disease has been identified in the glycogen branching enzyme 1 gene (*GBE*1) as a cytosine to adenosine substitution at base 102 that results in a tyrosine to stop mutation in codon 34 of exon 1.[7] Homozygous foals are either stillborn, die shortly after birth, or are euthanized within the first few months of life due to worsening clinical signs. Clinical signs vary and may include progressive muscle weakness, hypoglycemic seizures, respiratory failure, or sudden death. A study performed to assess the carrier frequency of this allelic mutation in populations of Quarter horses and Paint horses estimated that 8.3% of Quarter horses and 7.1 % of Paint horses are heterozygous for the mutated form of *GBE*1.[4]

Normal glycogen is present in the cytosol in the form of small electron dense granules that range in diameter from 10 to 40 nm and are comprised of glucose molecules that have α 1, 4 linkages between glucose residues and α 1, 6 glycosidic bonds at every 10th residue that create a branched polymer.[3] Branching of the polymer increases water solubility and provides a larger number of terminal residues which are the sites for enzymatic action of glycogen phosphorylase and glycogen synthase; enzymes that are responsible for glycogen degradation and synthesis, respectively. While glycogen synthase catalyzes the synthesis of α-1, 4 linkages between glucose residues, glycogen branching enzyme is responsible for the formation of the α 1, 6 glycosidic bonds that create the branched form of the glucose polymer, glycogen. Animals born deficient of this enzyme form non-branching, PAS-positive, diastase-resistant glucose polymers that form large aggregates within the cytoplasm of various tissues including skeletal muscle, brain, spinal cord, heart, liver. Glucose polymers that have only α -1, 4 linkages between glucose residues or those having few α-1, 6 glycosidic bonds (1 per 30 glucose residues) are amylose and amylopectin, respectively.[3] Amylose and amylopectin are starches that serve as nutritional reservoirs for plants and are not normal storage forms of glucose in mammalian species. Glycogen branching enzyme deficiency (equine glycogen storage disease IV) has previously been termed "amylopectinosis" prior to identification of the genetic mutation responsible for this disease.[2] Also, prior to discovering the genetic mutation and inheritance pattern, Valberg, et al. reported that glycogen branching enzymatic activity was virtually absent in affected foals and that some of the half-siblings of the affected foals

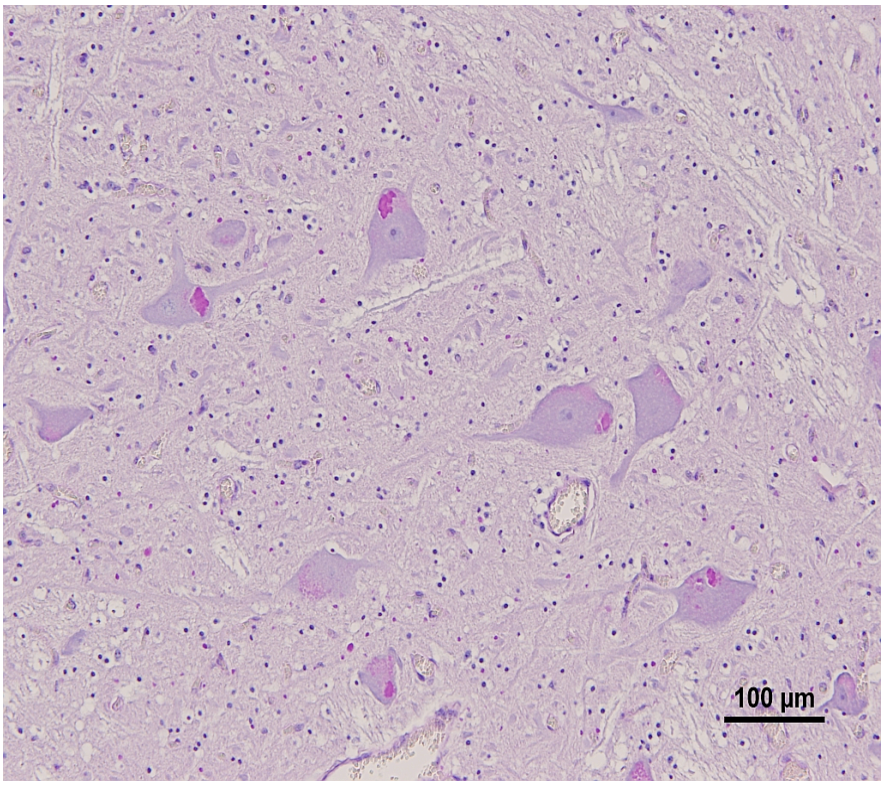

4-5. Brainstem foal: Brainstem inclusions are also PAS-positive. (PAS 200X) (Photo courtesy of: University of California, Davis, Veterinary Medical Teaching Hospital, VM3A, Anatomic Pathology, One Shields Avenue, Davis, CA 95616 http://www.vetmed.ucdavis.edu/pmi/)

had an approximately 50% decrease in GBE activity.[6]

The breed of the foal (Quarter horse) and the character and staining properties of the numerous intracytoplasmic inclusions seen within all examined skeletal muscles, heart, and brainstem were consistent with glycogen branching enzyme deficiency, also referred to as glycogen storage disease IV. This diagnosis was confirmed by genotype analysis. The hemorrhages seen in multiple organs are considered agonal. The partial aeration of the lung parenchyma may have occurred during attempts at resuscitation or at the time of parturition when the foal was reported to have gasped for air prior to ceasing to breathe.

JPC Diagnosis: 1. Skeletal muscle: Glycogen-like inclusions, intrasarcoplasmic, many, with multifocal mild rhabdomyocyte degeneration.
2. Cardiac muscle: Glycogen-like inclusions, intrasarcoplasmic, many.
3. Brainstem, gray matter, neurons: Glycogen-like inclusions, intracytoplasmic, rare.

Conference Comment: The contributor adeptly describes the pathogenesis behind the defect in glycogen metabolism and formation of inclusions in this important entity of American quarter and paint horses as well as Norwegian forest cats. Glycogen is a crucial source of energy stored in myocytes and in variable amounts within hepatocytes. When glucose is found in excess, it is converted into glycogen and stored in hepatocytes, thus glycogen concentration within the liver is highest shortly after eating, or in animals with abnormal glucose metabolism such as those with diabetes. Renal tubular epithelial cells and B-cells of the islets of Langerhans also can convert glucose to glycogen, resulting in intracellular accumulation in diabetics.[1]

Glycogen is demonstrated histologically using the PAS reaction on two serial sections. Pretreatment of one section with diastase enables its comparison between the intensity of magenta staining of the two sections to determine whether glycogen is present. If glycogen is present, diastase will digest it and remove it from the tissue (diastase-sensitive), thus removing the magenta color. The inclusions in this case are diastase-resistant because, as the contributor describes, the deficient glycogen branching enzyme (GBE) is necessary to form the glycosidic bonds between glucose molecules, creating the branching polymer glycogen. This is in contrast to other glycogen storage diseases such as type I and III which involve deficiencies in the conversion of glycogen to glucose, thus resulting in excess accumulation of glycogen.[1] All types of glycogen storage diseases are characterized by defects in the glycogen metabolic pathway and ultimately result in the failure of adequate utilization of energy resources leading to generalized muscle weakness or death.

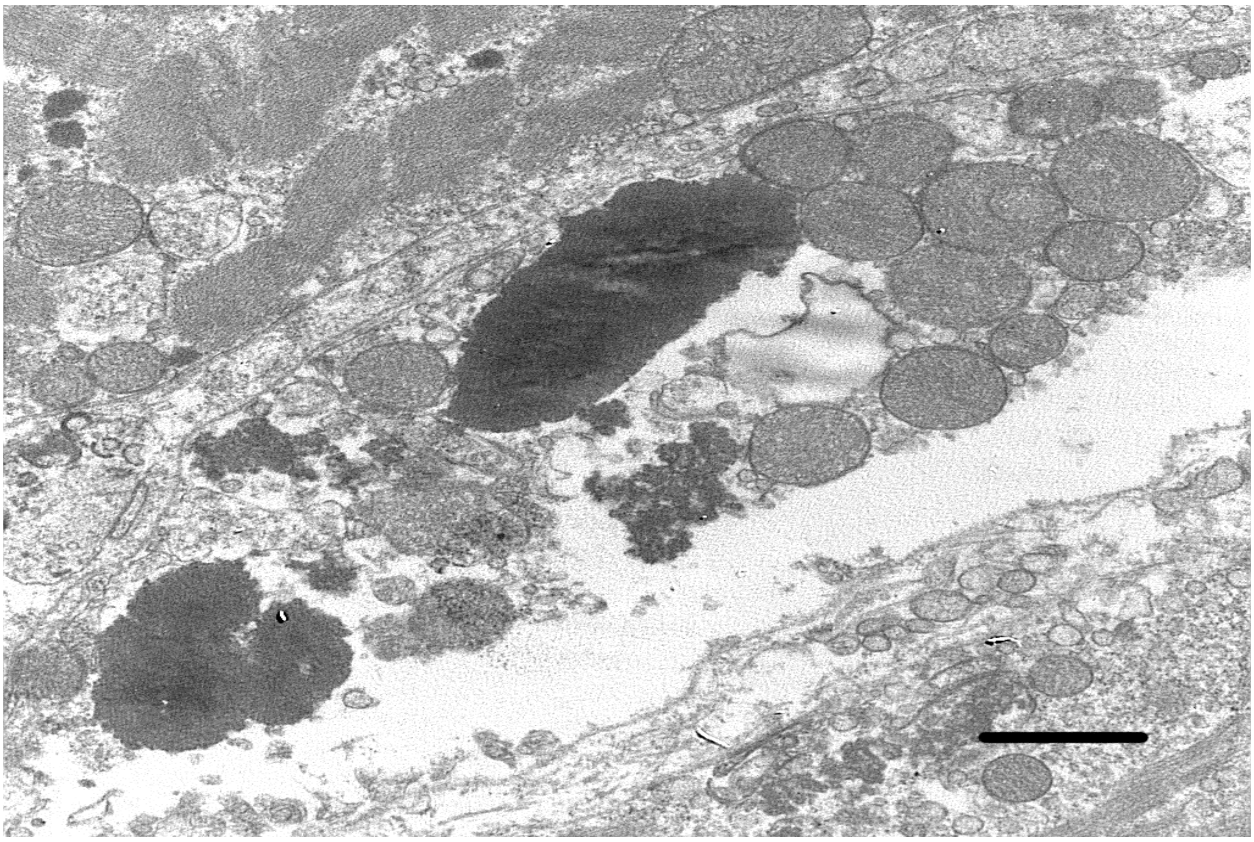

4-6. Skeletal muscle, foal: Transmission electron micrograph of formalin fixed skeletal muscle showing large electron dense intracytoplasmic inclusions within a degenerate skeletal muscle fiber. Bar = 1 µm (Photo courtesy of: University of California, Davis, Veterinary Medical Teaching Hospital, VM3A, Anatomic Pathology, One Shields Avenue, Davis, CA 95616 http://www.vetmed.ucdavis.edu/pmi/).

Another storage myopathy commonly recognized in the American Quarter horse, though reported in many other breeds, is equine polysaccharide storage myopathy. A definitive abnormality of the glycolytic or glycogenolytic pathway has not yet been identified for this entity, although a point mutation in skeletal muscle glycogen synthase I (GYS1) gene has been associated with some cases. This disease results in the accumulation of intracytoplasmic glycogen within type 2 fibers, which can become amylase-resistant inclusions as the glycogen becomes ubiquitinated in chronic cases. Episodes of exertional rhabdomyolysis is often associated with this condition.[5]

A second major group of storage diseases worthy of mention in domestic animals are those of lysosomes, characterized by a deficiency of lysosomal acid hydrolases leading to the excess accumulation of insoluble metabolites within lysosomes. For a case example and in-depth discussion of the numerous types of lysosomal storage diseases, we refer the reader to WSC 2013 (conference 5, case 2).

Contributing Institution: University of California, Davis
Veterinary Medical Teaching Hospital, VM3A, Anatomic Pathology
One Shields Avenue
Davis, CA 95616
http://www.vetmed.ucdavis.edu/pmi/

References:

1. Myers RK, McGavin MD, Zachary JF. Cellular adaptations, injury and death: Morphologic, biochemical, and genetic bases. In: Zachary JF, McGavin MD, eds. *Pathologic Basis of Veterinary Disease*. 5th edition. St. Louis, MO: Elsevier Mosby; 2012:35,54-55.
2. Render JA, et al. Amylopectinosis in a fetal and neonatal Quarter horse. *Vet Pathol*. 1999;36:157-160.
3. Stryer L. *Biochemistry*. 4th edition. New York: WH Freeman and Company; 1995:472-473, 581-588.
4. Valberg SJ, et al. Glycogen branching enzyme deficiency in Quarter horse foals. *J Vet Intern Med.* 2001;15:572- 580.

5. Valentine BA, McGavin MD. Skeletal muscle. In: Zachary JF, McGavin MD, eds. *Pathologic Basis of Veterinary Disease*. 5th edition. St. Louis, MO: Elsevier Mosby; 2012:902-904.
6. Wagner ML, et al. Allele frequency and likely impact of the glycogen branching enzyme deficiency gene in Quarter horse and Paint horse populations. *J Vet Intern Med* 2006;20:1207-1211.
7. Ward TL, et al. Glycogen branching enzyme (*GBE1*) mutation causing equine glycogen storage disease IV. *Mamm Genome* 2004;15:570-577.